Position/Force Control Using a 6-axis Compliance Device with Force/Torque Sensing Capability

Han Sung Kim
Kyungnam University/Mechanical Engineering, Changwon, Korea
Email: hkim @kyungnam.ac.kr

***Abstract*—In this paper, the position/force control algorithm using a 6-axis compliance device with force/torque sensing capability is investigated. Differently from the traditional methods using strain gage-type force/torque sensor with very small compliance, this control method uses a compliance device to provide enough compliance between robot and rigid environment. This control method is to simply control the position of a working robot's end-effector with the total twist of compliance in (13). The position/force control algorithm and control hardware system are developed. A simple design method of a compliance device with diagonal stiffness matrix is presented. The effectiveness has been verified through position/force control experiments.**

***Index Terms*—compliance device, force/torque sensor, position/force control**

I. Introduction

Currently, most industrial robots rely on only position control capability. It is well known that accurate force control as well as position control is required to complete the tasks such as peg in hole with very small tolerance, fastening bolts, grinding, deburring, etc.

Hybrid position/force control method is usually applied for the force control tasks. However, the method is based on the assumption that force control direction (wrench of constraint) and position control direction (twist of freedom) are orthogonal to each other [1], [2]. This method can be applied only when stiffness matrix between a working robot and an environment becomes diagonalized. Another approach is to use RCC (Remote-Center-of-Compliance) mechanism [3]. However, task should be performed only at the center of compliance. In order to resolve the problems, Griffis and Duffy [4]-[6] presented a novel and general position/force control theory to decompose position/force control directions which are orthogonal with respect to stiffness matrix. A few research results on the design of compliance devices have been published [7]-[9]. However, position/force control experiment results using compliance devices have been very limited [6].

In this paper, position/force control algorithm using a 6-axis compliance device is developed based on the control theory [4]-[6]. A simple design method of a 6-axis compliance device having decoupled stiffness is presented. The control hardware system including a 6-DOF parallel robot, a 6-axis compliance device, and PC-based controller with xPC Target is developed. Finally, two kinds of position/force control experiments (1DOC-5DOF and 3DOC-3DOF) have been performed to verify the effectiveness of the developed control algorithm, where DOC and DOF mean the numbers of force and position controlled directions, respectively.

Manuscript received July 1, 2013; revised February 10, 2014.

II. Position/Force Control Algorithm

As shown in Fig. 1, the position/force control is to simultaneously control displacement and force between the tool of a robot and workpiece by using a compliance device mounted on the end-effector of a robot.

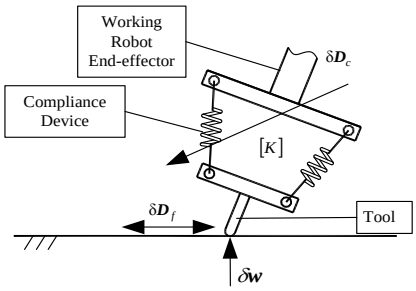

Figure 1. Illustration of the position/force control.

The position/force control scheme can be briefly explained as follows: The position and force controlled directions are defined here as twists of freedom, δD_f, and wrenches of constraint, δw, which are equivalent to the artificial constraints in the hybrid control [2]. It is noted that the twists of freedom and the wrenches of constraint should satisfy the reciprocal relation given by

$$\delta D_f^T \delta w = 0 \tag{1}$$

In this paper, $\delta D = [\delta p^T, \delta\theta^T]^T$ denotes a twist in axis coordinates, where δp and $\delta\theta$ are infinitesimal linear and rotational displacements. And $w = [f^T, n^T]^T$ denotes a wrench in ray coordinates, where f and n are force and moment vectors.

For a given task, the wrench acting on the workpiece can be controlled by the motion of the end-effector of a robot, δD_c, called twists of compliance (or force

doi: 10.12720/joace.3.1.35-39

controlled direction). The twists of compliance, δD_c, required for δw can be obtained through the inverse of a stiffness matrix, K^{-1} (refer to Fig. 1).

$$\delta D_c = -K^{-1}\delta w \tag{2}$$

Since the reciprocity relation $\delta D_f^T K \delta D_c = 0$ obtained from Eqs. (1) and (2) holds, this position/force control is to decompose the motion of a working robot into δD_f and δD_c.

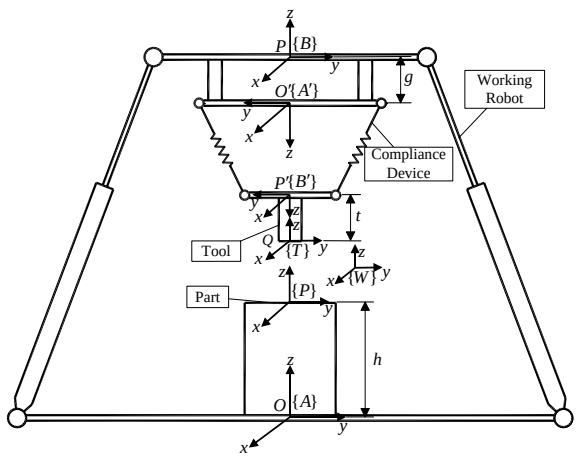

Figure 2. Definition of frames.

Fig. 2 shows a compliance device attached at the Gough-Stewart platform parallel-kinematic working robot and the definition of frames required to derive the control algorithm. In this paper, the parallel robot is used just as a positioning source. It is noted that this compliance device can be also mounted at the end-effector of an industrial serial-kinematic robot. Even for a serial-kinematic robot, this control algorithm can be applied in the same manner.

In this paper, all the reference inputs and actual values of position and force are expressed with respect to the work frame $\{W\}$, first. Then the position and force errors are transformed to the instantaneous frame of the working robot, $\{C\}$ in order to control the position of the moving platform (or end-effector) of the working robot. The frame $\{C\}$ locates at point B and has the axes parallel to those of frame $\{A\}$ (see Fig. 2). The leading superscript denotes a frame in which a vector or matrix is expressed. The twist and wrench in frame $\{j\}$ are transformed to those in frame $\{i\}$ by introducing rigid body transformations,

$$^{i}\delta D = {}^{i}[E]_j \, {}^{j}\delta D, \; ^{i}w = {}^{i}[e]_j \, {}^{j}w \tag{3}$$

with

$$^{i}[E]_j = \begin{bmatrix} ^{i}R_j & ^{i}p_{ij} \times {}^{i}R_j \\ 0_{3\times3} & ^{i}R_j \end{bmatrix}, \; ^{i}[e]_j = \begin{bmatrix} ^{i}R_j & 0_{3\times3} \\ ^{i}p_{ij} \times {}^{i}R_j & ^{i}R_j \end{bmatrix} \tag{4}$$

where $^{i}R_j$ is the rotation matrix from $\{j\}$ to $\{i\}$ and $^{i}p_{ij} \times$ is the vector in frame $\{i\}$ from origin $\{i\}$ to origin $\{j\}$ expressed as a 3×3 skew-symmetric matrix.

The proposed position/force control algorithm is presented in Fig. 3, where I.K., J_{WR}^T, and D_R denote the inverse kinematics, Jacobian matrix, and reference trajectory of the working robot, respectively. The procedure to calculate the twists of freedom and compliance in frame $\{C\}$ can be summarized as follows.

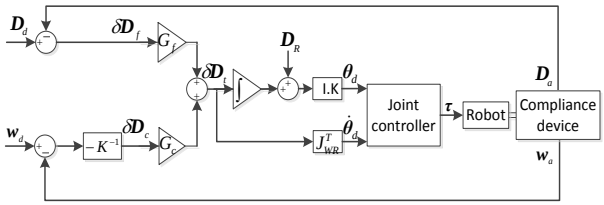

Figure 3. Block diagram of the position/force control.

First, the twist of freedom (or position error vector) in the work frame can be calculated by

$$^{W}\delta D_f = {}^{W}D_d - {}^{W}D_a \tag{5}$$

where $^{W}D_d = 0_{6\times1}$ and $^{W}D_a$ denote the desired and actual tool positions in frame $\{W\}$, where D_a can be calculated by the forward kinematics of the working robot and the compliance device with corresponding measured joint encoder values. Then, the twists of freedom in frame $\{C\}$ is calculated by

$$^{C}\delta D_f = {}^{C}[E]_W \, {}^{W}\delta D_f \tag{6}$$

Second, wrenches of constraint (or force error vector) and twists of compliance by stiffness mapping can be obtained by the following procedures. The actual (or measured) wrench is calculated by the statics relation.

$$^{A'}w_a = {}^{A'}J\tau \tag{7}$$

where $^{A'}J$ is the Jacobian matrix expressed in the fixed frame of the compliance device $\{A'\}$, $\tau = [\tau_1, L, \tau_6]^T$, and $\tau_i = k_i(l_i - l_{0i})$ where k_i is the spring constant, and l_i and l_{0i} the measured and initial spring lengths of the ith leg in a compliance device. The actual wrench in frame $\{W\}$ can be expressed by

$$^{W}w_a = {}^{W}[e]_{A'} \, {}^{A'}w_a \tag{8}$$

The force error vector is given by

$$^{W}\delta w = {}^{W}w_d - {}^{W}w_a \tag{9}$$

where $^{W}w_d$ denotes a desired input wrench. Since the Jacobian and stiffness matrices are expressed in frame $\{A'\}$, the force error vector needs to be transformed to the frame,

$$^{A'}\delta w = {}^{A'}[e]_W \, {}^{W}\delta w \tag{10}$$

where $^{A'}[e]_W = {}^{W}[e]_{A'}^{-1}$. The twists of compliance corresponding to the wrenches of constraint (or force error vector) can be obtained from the stiffness mapping

$$^{A'}\delta D_C = -{}^{A'}K \, {}^{A'}\delta w \tag{11}$$

Then, the twist of compliance in frame $\{C\}$ is given by

$$^{C}\delta D_c = {}^{C}[E]_{A'} \, {}^{A'}\delta D_c \tag{12}$$

where $^{C}[E]_{A'}$ is the screw transformation matrix from $\{A'\}$ to $\{C\}$ whose columns are expressed in axis coordinates.

Finally, the total twist of compensation is obtained by the sum of twists of freedom and compliance multiplied by scalar gains by

$$^{C}\delta D_t = G_f \, {}^{C}\delta D_f + G_c \, {}^{C}\delta D_c \tag{13}$$

where G_f and G_c are the position and force gains.

III. Compliance Device Design

It is noted that the proposed control method does not require the center of compliance or a diagonal stiffness matrix. However, in order to reduce coupling effects among axes, it is desired to design a diagonal stiffness matrix. In order to design a 6-axis compliance device with a diagonal stiffness matrix, adjacent legs need to be perpendicular to each other as shown in Fig. 4(b). For example, the unit direction of leg 1 should satisfy the following conditions at an initial position.

$$s_{1x} = \frac{r_b \cos\phi_b - r_a \cos(\pi/3 - \phi_a)}{l_0} = 0 \,,$$

$$s_{1y} = \frac{r_b \sin\phi_b - r_a \sin(\pi/3 - \phi_a)}{l_0} = -\frac{1}{\sqrt{2}} \,, \quad s_{1z} = \frac{h_0}{l_0} = \frac{1}{\sqrt{2}}$$

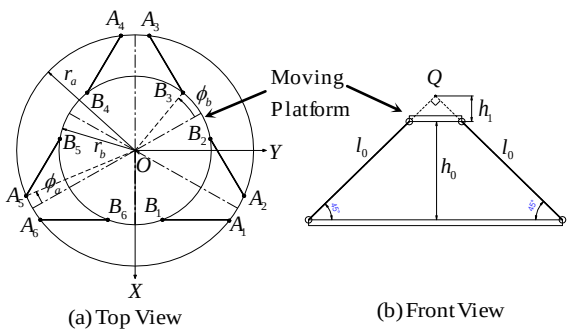

Figure 4. Geometry of a parallel kinematic mechanism.

When l_0 , ϕ_a , and ϕ_b are selected with practical considerations, h_0 , r_a and r_b can be determined by

$$h_0 = l_0 / \sqrt{2} \,,$$

$$r_a = (l_0/\sqrt{2})\cos\phi_a \sec(\phi_a + \phi_b + \pi/6) \,, 0.$$

$$r_b = (l_0/\sqrt{2})\sin(\phi_a + \pi/6)\sec(\phi_a + \phi_b + \pi/6)$$

Table I shows the design result for given l_0 , ϕ_a , and ϕ_b . The Cartesian stiffness matrix at the center of compliance, $Q\,(h = 17\text{mm})$ is given by

$$K = k \times diag\left(\frac{3}{2}, \frac{3}{2}, 3, \frac{3r_b^2}{2}, \frac{3r_b^2}{2}, 3r_b^2\right)$$

Each leg of the compliance device has a linear spring with spring constant of $k = 6.5$ N/mm mounted in the cylinder and a linear optical encoder with 5μm resolution. The ideal force resolution of each leg is 32.5mN and linear force resolution of the compliance device along the x- and y-axes is about 39mN and one along the z-axis is about 138mN. It is noted that for large deformation, the stiffness matrix becomes asymmetric and its derivation can be found in [10]. Based on the design results, a prototype 6-axis compliance device with linear optical encoders is shown in Fig. 5.

TABLE I. Design Results of the 6-Axis Compliance Device.

Kinematic Parameters	Value
Initial leg length (l_0)	135.5 mm
Half angle at the fixed platform (ϕ_a)	6.9 °
Half angle at the moving plate (ϕ_b)	11.3 °
Radius of the fixed platform (r_a)	140.962 mm
Radius of the moving platform (r_b)	86.309mm
Initial height of the moving plate (h_0)	95.813 mm
Maximum spring deflection	±10.0 mm

Figure 5. Prototype of a 6-axis compliance device with force/torque sensing capability.

IV. Experiment Results

A. Experimental Setup

As shown in Fig. 6, the 6-DOF Gough-Stewart platform is used as a working robot and the 6-axis compliance device is mounted under the moving platform of the working robot. Table II presents the specification of the working robot. The control system consists of a Host PC, a Target PC with DAQs, 6 AC servo drivers and interface boards. The control program is made with Simulink and xPC Target from MathWorks.

Even if several position/force control cases are possible, only two cases (1DOC-5DOF and 3DOC-

3DOF) have been experimented as shown in Fig. 7 to verify the feasibility of the proposed control algorithm and gain effects, where DOC and DOF denote degree-of-constraint and degree-of-freedom.

TABLE II. SPECIFICATION OF THE PARALLEL WORKING ROBOT.

Kinematic Parameters	Value
Radius of the fixed platform (r_a)	496.040 mm
Radius of the moving platform (r_b)	255.376 mm
Half angle at the fixed platform (ϕ_a)	4.046 °
Half angle at the moving platform (ϕ_b)	8.223 °
Min. length of actuators ($l_{\min}$)	668 mm
Max. length of actuators ($l_{\max}$)	979 mm
Stroke of actuators (Δl)	311 mm

B. Experiment for 1DOC-5DOF Case

The first experiment is to control the force along the z-axis and to control the positions, $p_x, p_y, \theta_x, \theta_y, \theta_z$. The cubic trajectory of p_y is generated between ±80 mm. Three cases with different position and force gains are tested to investigate the effects of G_f and G_c .

Desired wrench: ${}^{W}w_d = [*,*,10;*,*,*]^T [N;Nm]$

Desired position: ${}^{W}D_{d0} = [0,\pm 80,*;0,0,0]^T [mm;rad]$

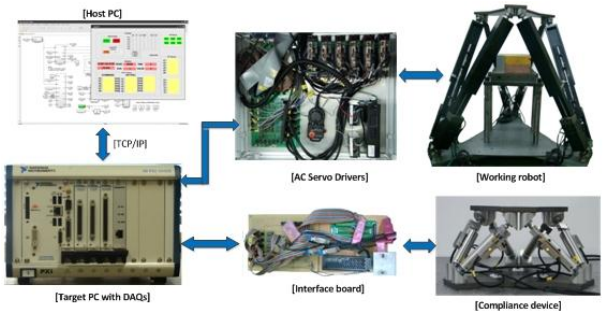

Figure 6. Configuration of the position/force control system.

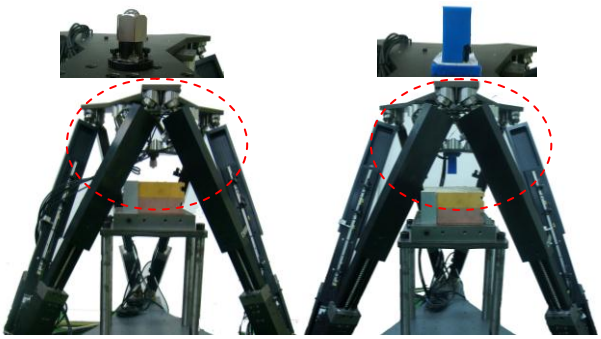

(a) 1DOC-5DOF (b) 3DOC-3DOF

Figure 7. Experimental setups.

where symbol * means that that position or force direction is not controlled. In the following figures, f_{tool} and n_{tool} denote the measured force and moment at the tool expressed in frame $\{W\}$, and p_{tool} and θ_{tool} denote the position and orientation of the tool expressed in frame $\{W\}$, which are corresponding to position and orientation errors.

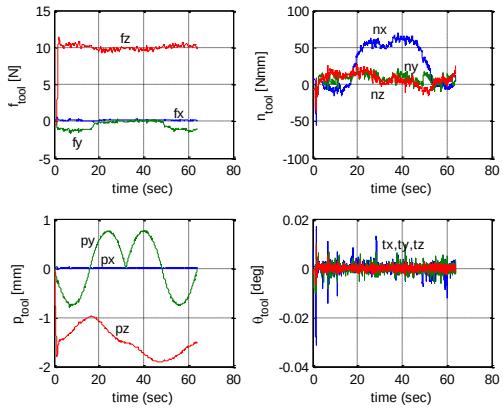

Figure 8. Case I: G_c = 0.025, G_f = 0.1.

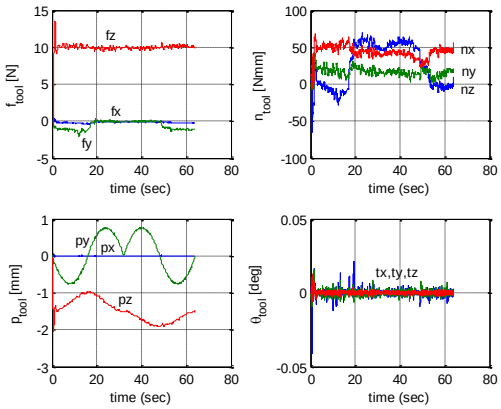

Figure 9. G_c = 0.05, G_f = 0.1.

First, the effect of G_c can be seen from Fig. 8 and Fig. 9.

- Case I: Smaller overshoot of f_z , slower response, larger force error.
- Case II: Larger overshoot of f_z , larger response, smaller force error.

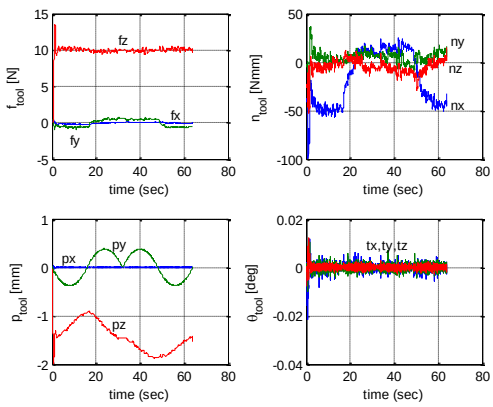

Figure 10. G_c = 0.05, G_f = 0.2.

Second, the effect of G_f can be seen from Fig. 9 and Fig. 10.

- Case II: Larger position tracking error.
- Case III: Smaller position tracking error.

In this experiment, only position and force gain effects are investigated. It is also noted that f_y is changing along the y-axis since unknown friction between the tool and work-piece exists.

C. Experiment for 3DOC-3DOF Case

In this experiment, force, f_z, and moments, n_x, n_y are controlled and positions, p_x, p_y, and orientation, θ_z are controlled. The cubic trajectory of p_y is also generated from 0 to 80 mm and from 80 to 0mm.

Desired wrench: ${}^{W}w_d = [*,*,10;0,0,*]^T [N;Nm]$

Desired position: ${}^{W}D_{d0} = [0,80,*;*,*,0]^T [mm;rad]$

It is noted that f_z, and n_x, n_y are regulated well and the friction force, f_y is not negligible as shown in Fig. 11.

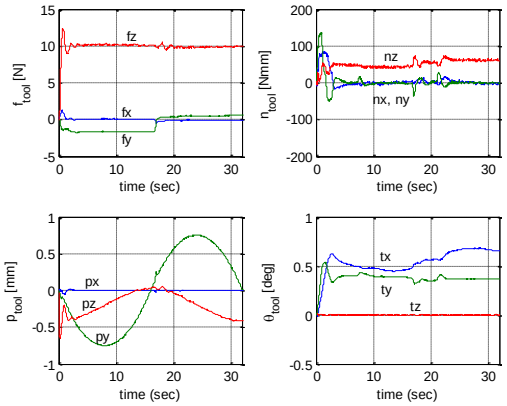

Figure 11. Experiment result with G_c = 0.05, G_f = 0.1.

V. Conclusions

The position/force control algorithm using a 6-axis compliance device is developed which can provide more compliance than using a strain gage-type force/torque sensor. A simple design method to yield a decoupled stiffness is presented and a prototype 6-axis compliance device with high force/torque sensing resolution is developed. Two kinds of position/force control experiments have been performed and the force as well as position follows the desired values well. However, the control should be performed with relatively low speed. Further works will focus on increasing control speed and developing more applications.

Acknowledgment

This work is partially supported by the project (No. 10041965) funded by the Korean Ministry of Trade, Industry and Energy.

References

[1] J. Duffy, "The fallacy of modern hybrid control theory that is based on orthogonal complements of twist and wrench spaces," *J. Robot. Syst.*, vol. 7, pp. 139-144, 1990.

[2] M. J. Raibert and J. J. Craig, "Hybrid position/force control of manipulators," *ASME J. Dyn. Syst. Meas. Contr.*, vol. 103, pp. 126-133, 1981.

[3] S. H. Drake and S. N. Simunovic, "Compliant assembly system device," U.S. Patent 4,155,169, 1979.

[4] J. Duffy, *Statics and Kinematics with Applications to Robotics*, Cambridge, UK: Cambridge University press, 1996, ch. 5 pp. 153-169.

[5] M. Griffis and J. Duffy, "Kinestatic control: A novel theory for simultaneously regulating force and displacement," *Trans. ASME Journal of Mechanical Design*, vol. 113, no. 4, pp. 508-515, 1991.

[6] M. Griffis, "A novel theory for simultaneously regulating force and displacement," Ph.D. dissertation, University of Florida, Gainesville, 1991.

[7] H. Jung, "Mechanisms with variable compliance," Ph.D. dissertation, University of Florida, Gainesville, 2006.

[8] S. W. Choi, Y. J. Choi, and S. H. Kim. "Using a compliant wrist for a teleoperated robot," in *Proc. IEEE/RSJ IROS*, 1991, pp. 585-589.

[9] T. Dwarakanath, C. Crane, J. Duffy, and C. Tyler, "In-Parallel passive compliant coupler for robot force control," in *Proc. ASME Mechanisms Conference*, Baltimore, Md., Sep 2000.

[10] M. Griffis and J. Duffy, "Global stiffness modeling of a class of simple compliant couplings," *Mechanisms and Machine Theory*, vol. 28, pp. 207-224, 1993.

Han Sung Kim Ph.D. degrees in Mechanical Engineering from Yonsei University, Seoul, Korea in 2000. He worked as a postdoctoral researcher at University of California, Riverside, USA from 2001 to 2003. He worked as a visiting professor at Georgia Tech, Atlanta, GA, USA from 2011 to 2012. Since 2004, he has been working as a professor in the School of Mechanical Engineering at Kyungnam University, Changwon, Korea. His research interests include mechanism design, kinematics, parallel robot applications, and MEMS.